Journal of Sound and Vibration (2001) **248**(5), 887–911
doi:10.1006/jsvi.2001.3827, available online at http://www.idealibrary.com on IDEAL®

NOISE LEVEL DISTRIBUTION FUNCTIONS FOR OUTDOOR APPLICATIONS

S. K. TANG AND S. H. K. CHU†

Department of Building Serivices Engineering, The Hong Kong Polytechnic University, Hong Kong, People's Republic of China. E-mail: besktang@polyu.edu.hk

(*Received* 21 *November* 2000, *and in final form* 30 *May* 2001)

In the present investigation, over 270 site measurements of noise levels are carried out in the Hong Kong residential areas. Results show that the noise climate is a good parameter for classifying the characteristics of the noise level time fluctuations. The relationships between percentile levels and the equivalent sound pressure levels are discussed and compared with results obtained from other cities. The log–tanh noise level cumulative distribution function proposed previously by the first author is found to be applicable in the outdoor situations provided that the noise environment is not dominated by limited strong noise events. This suggests the generality of this function for use in the environmental noise study.

1. INTRODUCTION

The noise outdoors has been investigated extensively in the past few decades. Many efforts have been concentrated on the setting up of prediction and control schemes, on the investigation of the noise characteristics and on the annoyance caused (for instance [1–4]). However, most of them are related to noise from traffic and a general picture of the outdoor noise characteristics has not yet been established even when one excludes the noise from construction and aircraft. Despite the efforts on traffic noise investigations, a general agreement on the noise level fluctuation distribution function has not yet been found though many proposals have been made (for instance [3– 6]). One should bear in mind that a predictable environmental noise level distribution not only enhances the study of the noise characteristics, but can enable a reasonable estimation of the noise climate, which is found to be significant in causing nuisance to humans [7, 8], in the planning stage. For time being, such a distribution function does not exist. The more relevant proposals are due to Don and Rees [6] and more recently to Tang and Au [9] for traffic noise, but they have not been widely adopted in the noise control field. A scheme for general environmental noise level distribution prediction appears far from reality.

Results of the recent studies of Tang [10] and Tang and Choy [11] have shown that the statistical distribution of the noise level fluctuations inside air-conditioned offices and canteens can be described by a set of long–tanh functions with the equivalent sound pressure level L_{eq} as the argument. The agreement between measurements and the predictions of these functions becomes more remarkable as L_{eq} increases. However, the

† Currently at FAR EAST Consulting Engineers Limited, Hong, Kong, People's Republic of China.

0022-460X/01/500887 + 25 $35.00/0

noises inside offices and canteens, though are intermittent in nature, are much more stationary than those in the outdoor environment. Also, the range of sound pressure level outdoors is considerably wider than that indoors. The level distribution functions applicable for indoor situations may not necessarily be able to describe what is happening outdoors.

In the present study, extensive site measurements of noise level fluctuations were carried out in the residential areas in Hong Kong. Noise from aircraft, trains and construction were excluded as they are relatively more impulsive and/or intermittent than those from vehicles and human activities. Their characteristics are left to future study. It is aimed at extending the use of the distribution functions of Tang [10] to the outdoor environment. It is also hoped that the present results can contribute to the establishment of a general noise level distribution function prediction scheme.

2. THE LOG–TANH DISTRIBUTION FUNCTION

The log–tanh cumulative distribution function C proposed by Tang [10] takes the form of

$$C(I) = \exp\{k_1\{\tanh[k_2(\log_e I + k_3)^{k_4}] - 1\}\}, \tag{1}$$

where I is the intensity ratio with the A-weighted equivalent sound intensity ($10^{L_{eq}/10}$) as the reference and k's are real numbers depending on L_{eq}. This function is developed using the data obtained from a large-scale survey in air-conditioned offices and its accuracy of prediction relies on the relationships between percentile levels and L_{eq}. The more linear the relationships, the better the predictions produced by equation (1). In general, this accuracy also increases with L_{eq} [11]. The constant k_1 has to be large enough so that $C \to 0$ for small I. As shown by Tang [10] and Tang and Choy [11], $k_1 = 10$ is sufficient to guarantee this convergence. Although C will not vanish theoretically according to equation (1), the noise levels associated with very small C are insignificant and are not of interest due to their extremely low occurrence levels. For large I, $C \to 1$. The probability density function $P(I)$ can be obtained by differentiating C with respect to I:

$$P(I) = \frac{\mathrm{d}C}{\mathrm{d}I} = \frac{k_1 k_4 C}{I} k_2 (\log_e I + k_3)^{k_4 - 1}\{1 - \tanh^2[k_2(\log_e I + k_3)^{k_4}]\}. \tag{2}$$

The values of k_2, k_3 and k_4 are determined using the sampled data. Details of the formulation of equation (1) and the comparisons between its performance with those of the other well-known functions, like the Pearson Type III [12] and Weibull distributions [13] can be found in Tang [10] and are not repeated here.

Similar to the Weibull distribution [13], the distribution in equation (1) is not developed from a concrete theoretical basis. The constants involved are also of unknown physical meanings, but they are expected to have relationships with the nature of the noise characteristics. However, the results of Tang and his co-worker [10, 11] have shown that such a distribution function performs better in predicting the noise level distributions indoors than the other established distributions. It will be shown later that it does give satisfactory estimations for the outdoor environment. The underlying theory and the physical meanings of the constants are left to further investigation.

It should be noted that the present proposed distribution will not give precisely the noise level cumulative or probability density distributions for a particular site with a particular L_{eq}. Rather, it gives general predictions to sites having similar characteristics with similar

L_{eq}'s. Similar logic can be found in other branches of acoustic predictions. The use of statistical energy analysis for sound transmission prediction in buildings is one of the examples [14].

3. SITE MEASUREMENTS

3.1. GENERAL INFORMATION

In the present study, 275 site measurements were carried out at 1 m from the façade of the residential buildings in Hong Kong. The major sources of noise are the ground traffic and human activities. The areas of measurements covered nearly all residential areas in Hong Kong with reasonable population densities. Each measurement was done by using the sound level analyzer Brüel & Kjær 2260 with a large logging capacity in good weather and when the wind speed was below 5 m/s. Sound pressure levels were recorded every second for at least 25 min during each measurement. The percentile levels and the noise level distributions were calculated from these time variations of sound pressure levels afterwards.

In order to describe the sites in more detail, the 275 sites surveyed in the present study are divided into 12 categories according to the location type and the degree to which the residents are affected by the noise from major roads or industrial areas as shown in Table 1. Such a classification is basically in-line with that adopted by the local authority. For those sites not affected by the two noise sources, one of the major noise sources will be the human activities. In fact, there are not many sites affected by the industrial noise directly as it is usually the trucks and container vehicles brought about by the industrial establishments that are really causing the noise. The last group of areas "Area other than the above" refer to those sub-urban areas but have significant population densities within a relatively large land area. Table 1 also summarizes the breakdown of sites into these 12 categories and the time periods of the measurements. Although there seems to be an imbalance in the number of sites surveyed in each category, it will be shown later that the site classification and the division of measurement time period as in Table 1 are not related to the noise characteristics obtained in the present study. A new form of classification is introduced in the next section.

TABLE 1

Details of site measurements

	Degree of Influence of Traffic and Industrial Estates[†]		
Area type	No effect	Indirect	Direct
Rural areas (villages and country park developments	EV01 D:5, E:8, N:8	EV02 D:6, E:6, N:6	EV03 D:8, E:5, N:5
Low-density residential area	EV04 D:5, E:5, N:5	EV05 D:4, E:4, N:7	EV06 D:8, E:8, N:5
Urban area	EV07 D:8, E:7, N:13	EV08 D:11, E:8, N:10	EV09 D:14, E:11, N:18
Areas other than the above	EV10 D:8, E:7, N:7	EV11 D:9, E:5, N:4	EV12 D:11, E:9, N:7

[†] D: Period 07:00–19:0 (day); E: Period 19:00–23:00 (evening); N: Period 23:00–07:00 (night).

3.2. RE-GROUPING OF DATA AND SITES

Figure 1 shows the relationships between the percentile levels, L_{10} and L_{90}, and L_{eq} obtained in the present study. All the 275 site measurement results are included. While a linear relationship between L_{10} and L_{eq} as in Tang [10] is observed, considerable scattering is found as far as L_{90} is concerned. Although some degree of scattering is expected at low percentile levels, the situation here is much worse than those in Tang [10] and Tang and Choy [11]. This reflects the high randomness of noise level fluctuations in the outdoor environment. Also, it is found that similar data scattering occurs even within the same site category specified by the scheme shown in Table 1. Some typical examples of this are shown in Figure 2, showing that the site classification scheme in Table 1 is not appropriate for environmental noise study. A new grouping scheme is required.

One can infer from Figure 1 that the data scattering for L_{90} may be due to the existence of more than one noise fluctuation characteristics/natures. Each of these characteristics lead to one particular set of k's. Such a phenomenon may not occur in an indoor environment where the noise level fluctuations are more stationary due to the characteristics of the noise sources and room reverberation [10, 11]. The scattering of L_{90} and the nearly linear relationship between L_{10} and L_{eq} result in scattering of the noise climates. Figure 3 illustrates the distribution of the noise climates at 1 dB intervals. The appearance of four peaks on the distribution tends to suggest that the overall distribution is formed from a minimum of four sub-distributions/groups. Each of these groupings will represent a certain type of noise level fluctuations. Similar peaks are also found in the distribution of $L_{50} - L_{90}$, which is a parameter discussed by Don and Rees [6], though are less distinct than those shown in Figure 3 (not shown here). Therefore in the present study, four groups of data are introduced and abbreviated by G1, G2, G3 and G4. G1 represents the group of data having $L_{10} - L_{90} \leqslant 6$ dB, G2 the group of data having 6 dB $< L_{10} - L_{90} \leqslant 9$ dB, G3 the group of data having 9 dB $< L_{10} - L_{90} \leqslant 14$ dB and G4 the group of data having $L_{10} - L_{90} > 14$ dB.

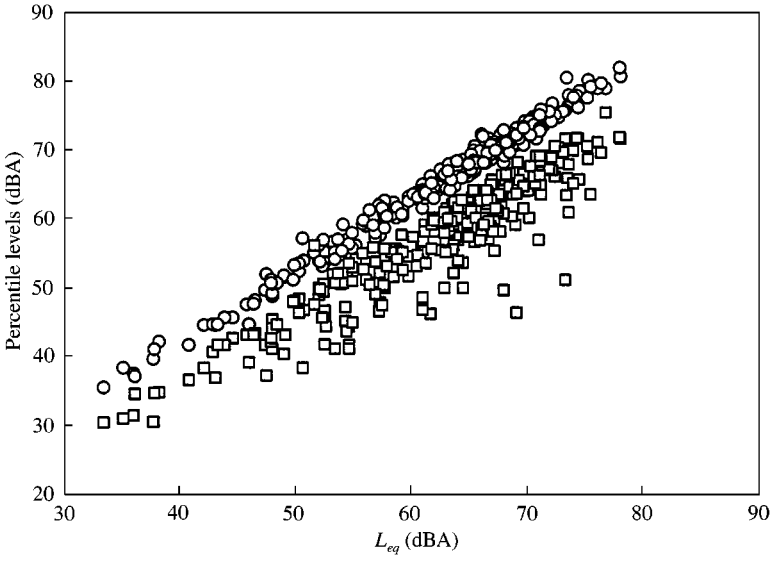

Figure 1. Overall relationships between percentile levels and L_{eq}. ○, L_{10}; □, L_{90}.

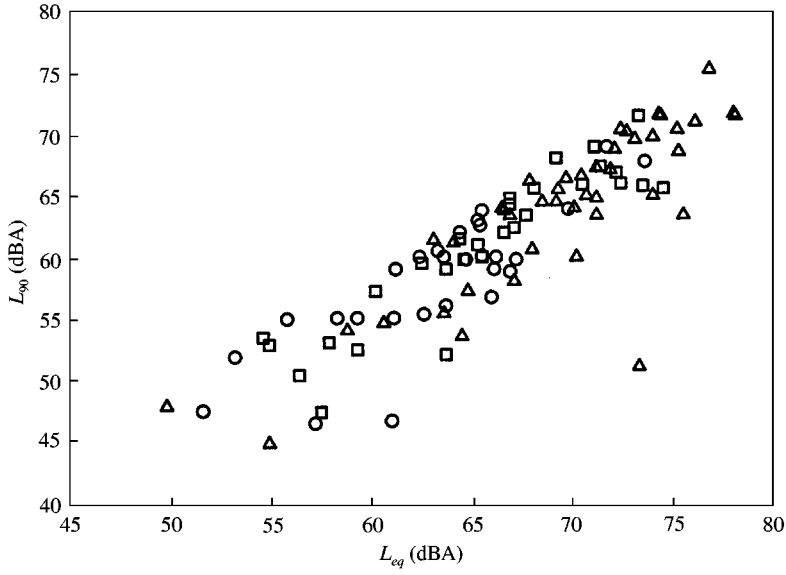

Figure 2. Examples of data scattering under site classification scheme described in Table 1: ○, EV07; △, EV08; □, EV09.

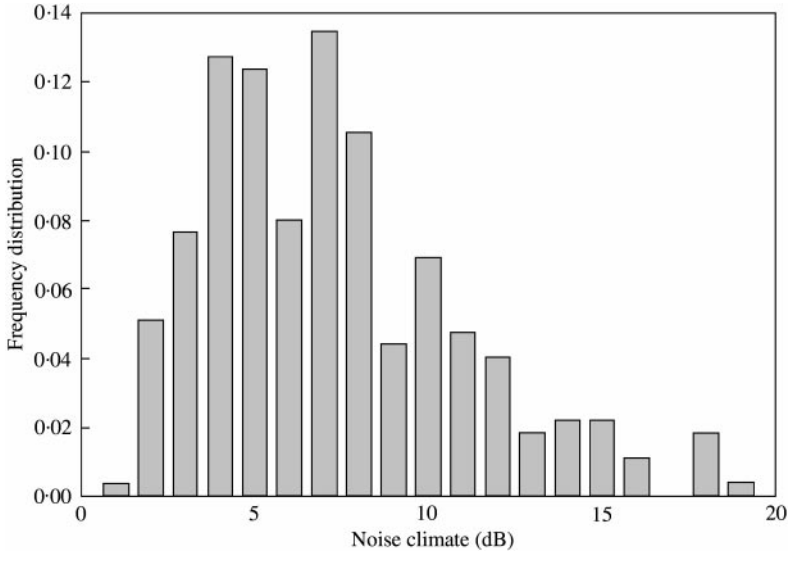

Figure 3. Distribution of noise climates.

In the present study, there are about 7% of the data having L_{eq} close to or even higher than L_{10}. They are obtained from sites with low background noise levels (usually at night-time or in rural areas). Figure 4 is a typical example of such data and the high L_{eq} is due to the occasional exposure of limited strong noise events. Such a phenomenon has also been observed by Bugress [15] in Australia. This type of noise has to be excluded from the present study as it is abnormal and is not representative. The parameter $(L_{eq} - L_{50})/(L_{10} - L_{50})$ is used here to verify the occurrence of such abnormality. Although this parameter cannot be found in existing literature, it is introduced in the present study to

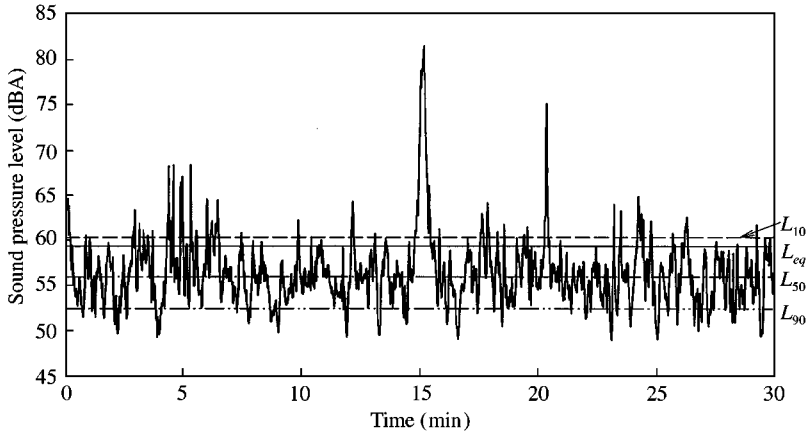

Figure 4. Example of a rejected noise level time fluctuation having L_{eq} very close to L_{10}. $(L_{eq} - L_{50})/(L_{10} - L_{50}) = 0{\cdot}77$.

TABLE 2

Mapping between the new grouping and that in Table 1

Site classifications in Table 1	G1 ($L_{10} - L_{90} \leqslant 6$)	G2 ($6 < L_{10} - L_{90} \leqslant 9$)	G3 ($9 < L_{10} - L_{90} \leqslant 14$)	G4 ($L_{10} - L_{90} > 14$)
EV01	D:1, E:0, N:1	D:1, E:1, N:4	D:1, E:2, N:0	D:0, E:3, N:1
EV02	D:1, E:3, N:2	D:2, E:2, N:2	D:2, E:1, N:1	D:0, E:0, N:0
EV03	D:1, E:1, N:1	D:2, E:2, N:2	D:4, E:1, N:1	D:0, E:1, N:1
EV04	D:1, E:1, N:4	D:0, E:2, N:1	D:2, E:1, N:0	D:1, E:0, N:0
EV05	D:1, E:3, N:3	D:2, E:0, N:2	D:0, E:1, N:0	D:0, E:0, N:1
EV06	D:2, E:3, N:1	D:3, E:4, N:1	D:3, E:0, N:2	D:0, E:1, N:1
EV07	D:2, E:4, N:6	D:2, E:1, N:2	D:4, E:2, N:3	D:0, E:0, N:1
EV08	D:3, E:3, N:4	D:4, E:4, N:3	D:4, E:0, N:1	D:0, E:0, N:2
EV09	D:4, E:6, N:4	D:9, E:3, N:3	D:1, E:2, N:10	D:0, E:0, N:1
EV10	D:3, E:2, N:3	D:4, E:4, N:1	D:0, E:1, N:1	D:0, E:0, N:1
EV11	D:3, E:3, N:1	D:5, E:0, N:1	D:0, E:1, N:2	D:1, E:0, N:0
EV12	D:6, E:5, N:2	D:3, E:3, N:3	D:2, E:1, N:2	D:0, E:0, N:0
Overall	D:28, E:34, N:32	D:37, E:26, N:25	D:23, E:13, N:23	D:2, E:5, N:9
Total number	94	88	59	16

indicate the position of L_{eq} relative to L_{10} in the noise cumulative statistics. The more positive this parameter, the higher the possibility of occurrence of the above-mentioned abnormality. For this example given in Figure 4, $(L_{eq} - L_{50})/(L_{10} - L_{50}) = 0{\cdot}77$. In the present data set, it is found that such abnormality is very likely to exist when

$$(L_{eq} - L_{50})/(L_{10} - L_{50}) \geqslant 0{\cdot}75.$$

The remaining number of valid noise level time fluctuations is 257. Certainly, one can use L_{90} instead of L_{50} in setting up the criterion for data rejection. However, the occasional strong noise events raise up L_{eq} toward or even above L_{10}. Therefore, it is believed that the use of L_{50} can give a better scaling on the magnitude of the abnormality.

Table 2 summarizes the mapping between the new grouping scheme and that given in Table 1. One can notice that while a majority of G4 noise level fluctuations is found during

night-time or evening and not within urban areas or sub-urban areas with significant population density, the opposite is observed for the G1 and G2 data. Over 40% of the G2 data are obtained during day-time within urban or sub-urban areas with significant population density. In the present study, about 70% of the noise climates are less than or equal to 9 dB. These statistics suggest that the present study deals with outdoor environments which are significantly different from those of Don and Rees [6] where a majority of noise climates are higher than 12 dB.

Figure 5 illustrates three typical examples of the noise level time fluctuations in the G1 group. In general, this group of noise level fluctuations is characterized by the presence of intermittent upward pointing spikes (bursts of noise). The low noise climates associated with these G1 noise level fluctuations are due to the existence of relatively intermittent noise sources with moderate strengths compared to the corresponding background noise levels. The time fraction for low noise level decreases as the noise climate increases. Such noise level time fluctuations are commonly found in areas with interrupted traffic flows [9].

The noise climate increases at noise event intermittence reduced as shown in Figure 6, which gives some typical examples of the G2 noise level fluctuations. It can be concluded

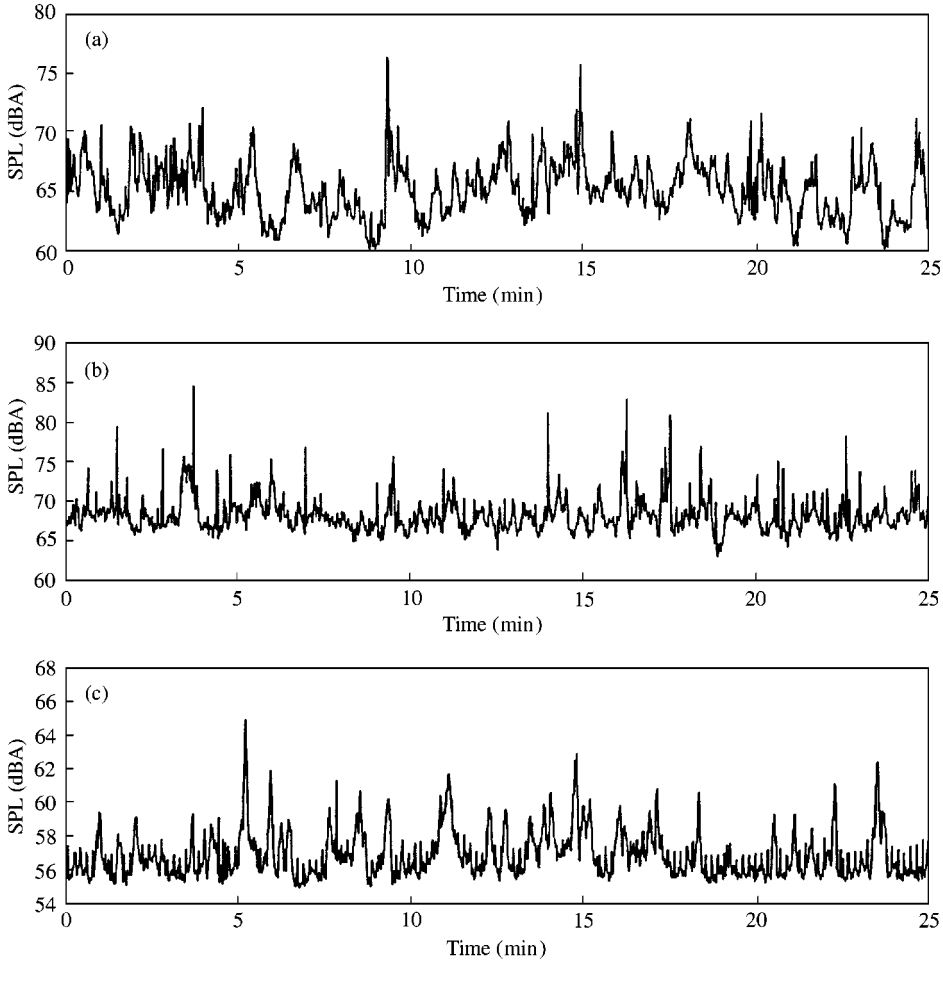

Figure 5. Examples of noise level time fluctuations for G1 data group.

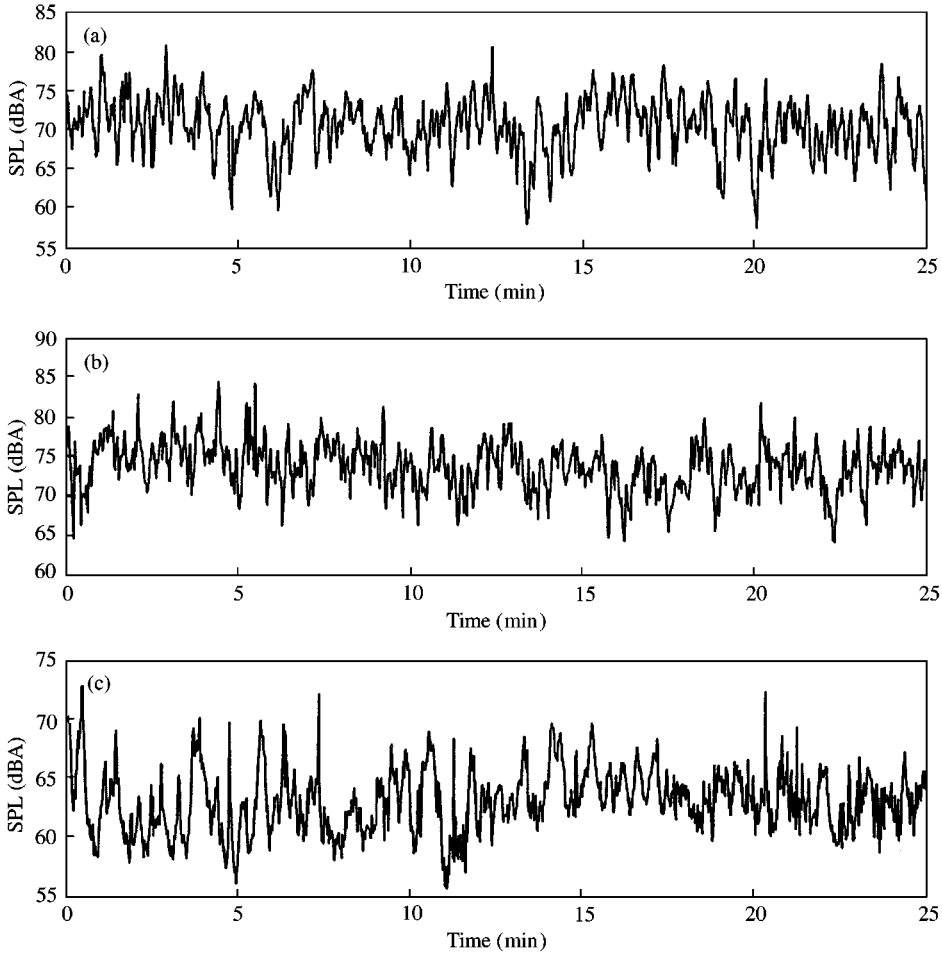

Figure 6. Examples of noise level time fluctuations for G2 data group.

that there exist relatively continuous incoherent noise sources and the noises they produced form the background noise at the sites. This type of noise level fluctuations is usually observed with free traffic flow [9]. When the noise climate is close to 6 dB, the noise level fluctuations resemble that shown in Figure 5(a) but with more regular bursts (Figure 6(c)).

Figure 7 illustrates the two dominating patterns of the G3 noise level fluctuations. The first type, which is shown in Figure 7(a), resemble that shown in Figure 6(a) but with significantly rapid large changes in the noise levels, resulting in large noise climate. Figure 7(b) shows a typical noise level fluctuation with periodically interrupted noise sources in a relatively quiet environment. This type of noise characteristics usually gives rise to a large noise climate with L_{eq} slightly higher than L_{50} and is usually found in areas with traffic light control [9]. The large noise climate with relatively low minimum noise level explains why most of the G3 noise level fluctuations are obtained during night-time and/or within areas directly affected by the noise sources (Table 2). The G4 noise level fluctuations are the extensions of G3 into the region of $L_{10} - L_{90} > 14$ (Figure 8). It can be observed that though the patterns of noise level fluctuations look similar to those shown in Figure 7, the duration of low noise level events for the G4 noise level fluctuations is longer. The large

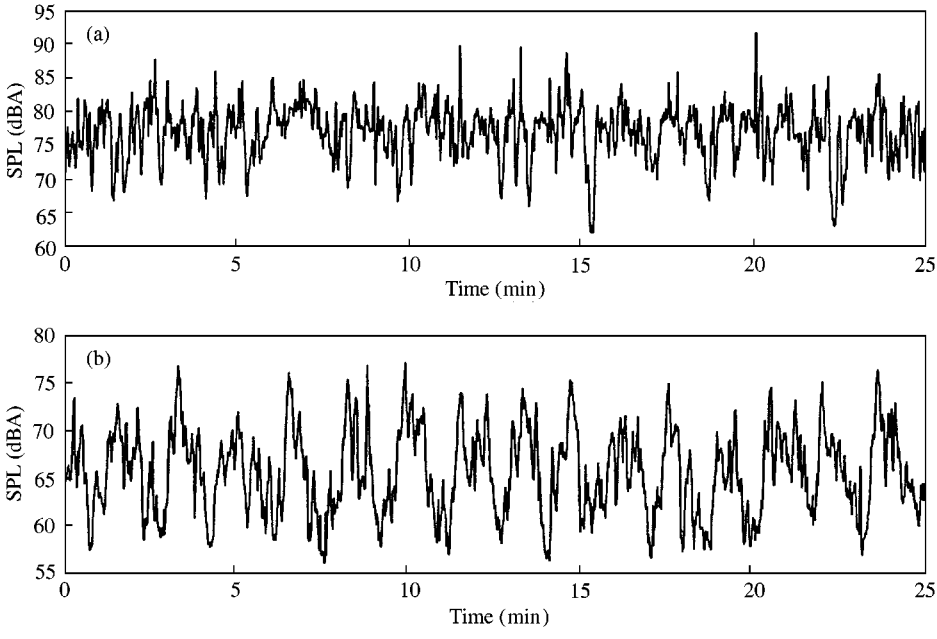

Figure 7. Examples of noise level time fluctuations for G3 data group.

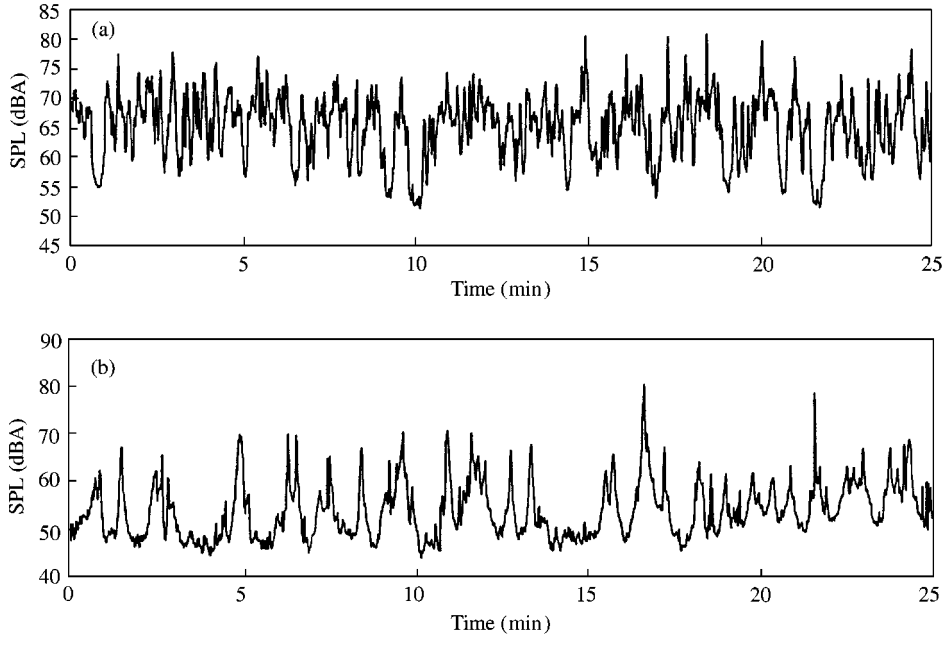

Figure 8. Examples of noise level time fluctuations for G4 data group.

noise climate and the increased importance of the low noise level events in the overall acoustical environment explain the observation in Table 2 that most of the G4 fluctuations are found in the rural or low population density areas during evening and night-time.

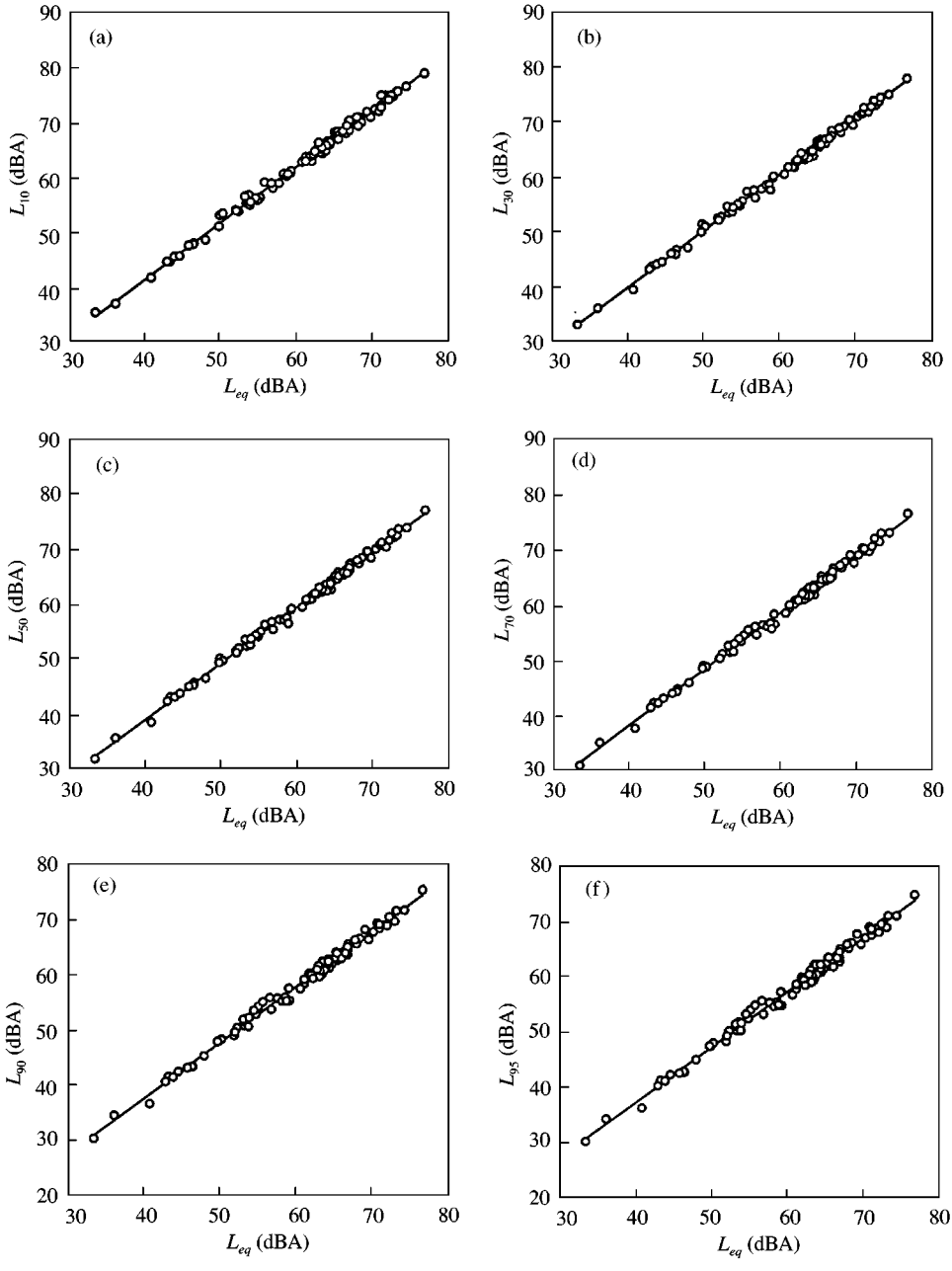

Figure 9. Linear relationships between percentile levels and L_{eq} and G1 data group. (a) L_{10}; (b) L_{30}; (c) L_{50}; (d) L_{70}; (e) L_{90}; (f) L_{95}: ——, regression lines; ○, measured data.

Although the pattern of noise level time fluctuations in Figure 8(b) resembles that in Figure 6(c), the appearance of much more regular noise bursts results in a much large noise climate. It is due to this periodicity that the L_{eq} in Figure 8(b) is likely half way between L_{10} and L_{50}.

It will be shown in the next section that the present data re-grouping scheme gives much more well-defined relationships between percentile levels and L_{eq} than those shown in

Figure 1. Together with the relatively distinct noise level fluctuation characteristics shown in Figures 5–8, the present re-grouping scheme is believed to be better than that described in Table 1.

4. NOISE DISTRIBUTION FUNCTIONS

4.1. G1 NOISE LEVEL FLUCTUATIONS

Noise level fluctuations in this G1 group are of relatively small noise climates. Figure 9 shows that linear relationships exist between some percentile levels L_N and L_{eq}. In fact, such linear relationships are observed for $5 \leqslant N \leqslant 95$. A summary of these linear relationships is given in Table 3. The correlation coefficients of all these relationships are all higher than 0·99, suggesting that equation (1) is applicable. Since the nature of noise in the present study is basically different from those of Tang [10] and Tang and Choy [11], the regression formulae shown in Table 3 are different from those listed in the two references. The uncertainty range (standard error) e is estimated by the procedure given in reference [16] at 95% confidence level. In general, this range is less than 0·2 dB but is still about 50% higher than those in Tang and Choy [11] obtained within a relatively noisy environment. The reliability of the prediction here is therefore expected to be lower than that in Tang and Choy [11].

Following the procedure of Tang [10], the values of k_2, k_3 and k_4 can be found once L_{eq} is fixed. Figure 10 shows a comparison between the predictions with measurements having $L_{eq} = 64{\cdot}4$ dBA. The corresponding values of k_2, k_3 and k_4 are 1·062, 1·535 and 1·296 respectively. As mentioned before, equation (1) is not expected to give an exact prediction for the cumulative distribution of the noise level fluctuations of a particular equivalent

TABLE 3

Summary of linear relationships between L_N and L_{eq} for G1 data

N	Regression formula	Correlation coefficient R^2	Uncertainty range e (dB)
5	$L_5 = 1{\cdot}005\, L_{eq} + 2{\cdot}757$	0·995	±0·18
10	$L_{10} = 1{\cdot}019\, L_{eq} + 0{\cdot}815$	0·997	±0·13
15	$L_{15} = 1{\cdot}022\, L_{eq} + 0{\cdot}017$	0·998	±0·12
20	$L_{20} = 1{\cdot}022\, L_{eq} - 0{\cdot}383$	0·998	±0·11
25	$L_{25} = 1{\cdot}023\, L_{eq} - 0{\cdot}785$	0·998	±0·11
30	$L_{30} = 1{\cdot}023\, L_{eq} - 1{\cdot}065$	0·998	±0·11
35	$L_{35} = 1{\cdot}023\, L_{eq} - 1{\cdot}329$	0·998	±0·11
40	$L_{40} = 1{\cdot}022\, L_{eq} - 1{\cdot}530$	0·998	±0·11
45	$L_{45} = 1{\cdot}022\, L_{eq} - 1{\cdot}699$	0·998	±0·11
50	$L_{50} = 1{\cdot}021\, L_{eq} - 1{\cdot}849$	0·998	±0·12
55	$L_{55} = 1{\cdot}020\, L_{eq} - 1{\cdot}996$	0·998	±0·12
60	$L_{60} = 1{\cdot}017\, L_{eq} - 2{\cdot}061$	0·998	±0·12
65	$L_{65} = 1{\cdot}016\, L_{eq} - 2{\cdot}196$	0·998	±0·12
70	$L_{70} = 1{\cdot}014\, L_{eq} - 2{\cdot}302$	0·998	±0·13
75	$L_{75} = 1{\cdot}012\, L_{eq} - 2{\cdot}388$	0·997	±0·13
80	$L_{80} = 1{\cdot}009\, L_{eq} - 2{\cdot}412$	0·997	±0·14
85	$L_{85} = 1{\cdot}007\, L_{eq} - 2{\cdot}532$	0·997	±0·14
90	$L_{90} = 1{\cdot}002\, L_{eq} - 2{\cdot}600$	0·997	±0·15
95	$L_{95} = 0{\cdot}994\, L_{eq} - 2{\cdot}591$	0·996	±0·17

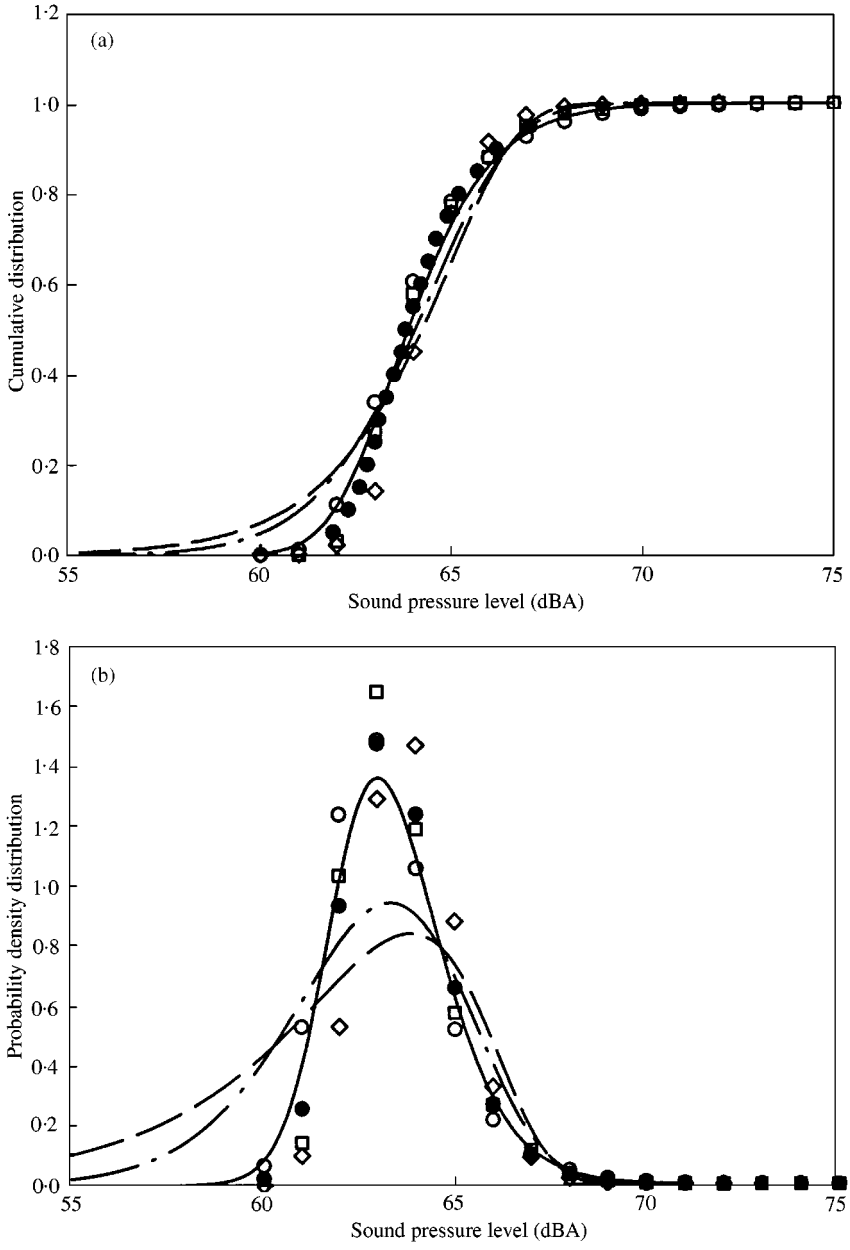

Figure 10. Example of a comparison between present model predictions and site measurements for G1 data. $L_{eq} = 64{\cdot}4$ dBA. (a) Noise level cumulative distribution; (b) noise level probability density distribution: ——, presented model; ○, □, ◇, measured results; ●, average of measured results; —·—, Pearson Type III distribution; — — —, Weibull distribution.

sound pressure level. The results shown in Figure 10(a) suggest that equation (1) can predict the average cumulative distribution within engineering tolerance. Although considerable data scattering is observed as far as the probability density distribution of the noise level fluctuations is concerned, the present model is able to predict the modes of the measured results with high accuracy. Again, the present model gives good prediction to the average

probability density distribution. In general, the performance of the proposed model (equations (1) and (2)) at other L_{eq}'s is similar to that shown in Figure 10, though slightly more deviations can be found towards the low end of the L_{eq} range due to the limited data available, and thus is not presented. In Figure 10, the results of fitting the Pearson Type III and the Weibull distributions to the present measured results are also shown. Since these two well-established distributions contain several unknowns, the fitting is done here by keeping L_{eq} and L_{10} the same as those estimated by using equations (1) and (2). It can be observed that these two distributions give rise to significant deviations from the measurements, especially on the low sound pressure level end of the statistics and predict lower kurtosis.

Figure 11 illustrates some examples of the probability density distributions calculated from equation (2) at different L_{eq}. It is noticed that the distributions become more positively skewed as L_{eq} decreases and the mode of each distribution is below the corresponding L_{eq}. This is consistent with the characteristics of these G1 noise level time fluctuations illustrated in Figure 5. The noise level distributions shown in Figure 11 belong to the Pearson Type I, IV and IV but are close to the Pearson Type III [12]. It is different from the results of Kurze [3] probably due to the fact that the noise sources here are not as continuous as those in Kurze [3].

4.2. G2 NOISE LEVEL FLUCTUATIONS

Figure 12 illustrates the linear relationships between L_N and L_{eq} for the G2 data. As shown in Table 4, the correlation coefficients are all higher than 0·99, but the uncertainties are slightly higher than those for the G1 noise level fluctuations. Figure 13

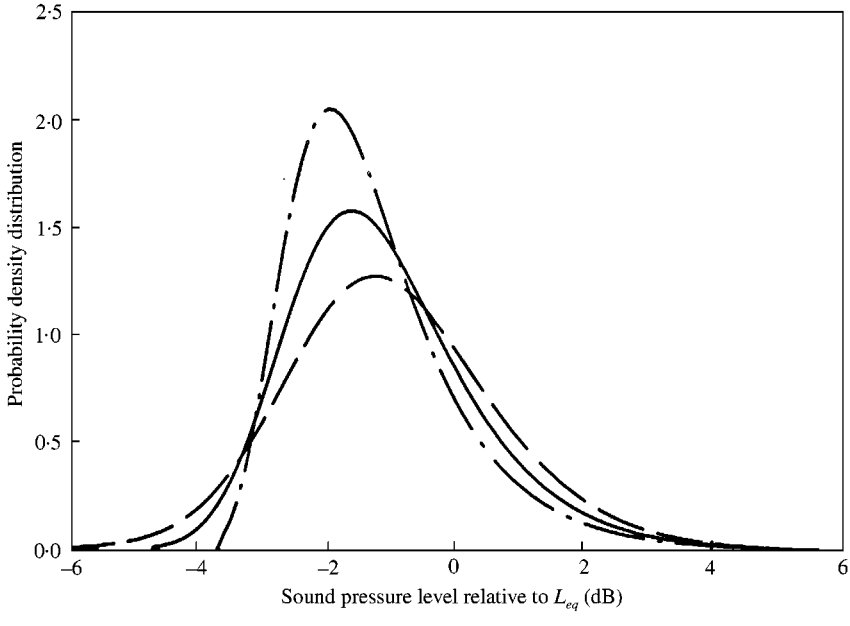

Figure 11. General trend of G1 data probability density distribution: —·—, $L_{eq} = 35$ dBA; ——, $L_{eq} = 52{\cdot}5$ dBA; – – –, $L_{eq} = 70$ dBA.

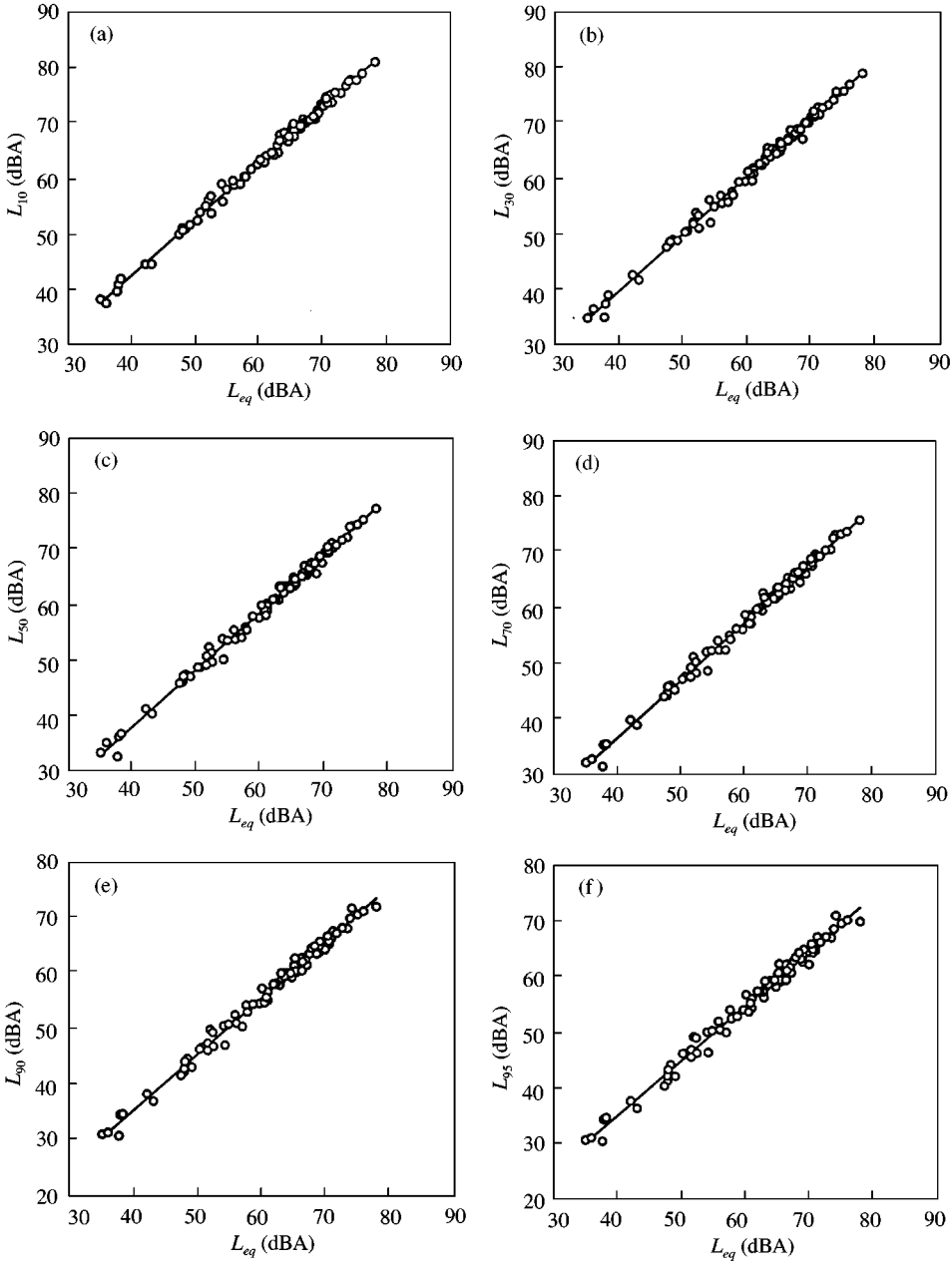

Figure 12. Linear relationships between percentile levels and L_{eq} and G2 data group. (a) L_{10}; (b) L_{30}; (c) L_{50}; (d) L_{70}; (e) L_{90}; (f) L_{95}: ——, regression lines; ○, measured data.

illustrates a comparison between predictions by equations (1) and (2) with actual site measurements at $L_{eq} = 47{\cdot}9$ dBA ($k_2 = 1{\cdot}146$, $k_3 = 1{\cdot}936$, $k_4 = 0{\cdot}874$). The deviations from the measured percentile levels are around 1 dB (Figure 13(a)), which is acceptable for environmental noise study. Equation (2) predicts correctly the modes of the measured noise level fluctuations but fails to give the actual spread of the distributions (Figure 13(b)). In general, the kurtosis of the G2 noise level fluctuation is lower than that in the

TABLE 4

Summary of linear relationships between L_N and L_{eq} for G2 data

N	Regression formula	Correlation coefficient R^2	Uncertainty range e (dB)
5	$L_5 = 0{\cdot}991\, L_{eq} + 4{\cdot}854$	0·996	±0·19
10	$L_{10} = 1{\cdot}010\, L_{eq} + 2{\cdot}258$	0·998	±0·15
15	$L_{15} = 1{\cdot}018\, L_{eq} + 0{\cdot}904$	0·998	±0·15
20	$L_{20} = 1{\cdot}023\, L_{eq} - 0{\cdot}086$	0·997	±0·16
25	$L_{25} = 1{\cdot}029\, L_{eq} - 0{\cdot}998$	0·997	±0·17
30	$L_{30} = 1{\cdot}032\, L_{eq} - 1{\cdot}685$	0·997	±0·17
35	$L_{35} = 1{\cdot}034\, L_{eq} - 2{\cdot}231$	0·997	±0·18
40	$L_{40} = 1{\cdot}034\, L_{eq} - 2{\cdot}630$	0·997	±0·18
45	$L_{45} = 1{\cdot}035\, L_{eq} - 3{\cdot}109$	0·997	±0·18
50	$L_{50} = 1{\cdot}035\, L_{eq} - 3{\cdot}431$	0·997	±0·18
55	$L_{55} = 1{\cdot}034\, L_{eq} - 3{\cdot}783$	0·997	±0·18
60	$L_{60} = 1{\cdot}033\, L_{eq} - 4{\cdot}047$	0·996	±0·19
65	$L_{65} = 1{\cdot}030\, L_{eq} - 4{\cdot}233$	0·996	±0·19
70	$L_{70} = 1{\cdot}027\, L_{eq} - 4{\cdot}395$	0·996	±0·19
75	$L_{75} = 1{\cdot}022\, L_{eq} - 4{\cdot}494$	0·996	±0·19
80	$L_{80} = 1{\cdot}018\, L_{eq} - 4{\cdot}652$	0·996	±0·19
85	$L_{85} = 1{\cdot}010\, L_{eq} - 4{\cdot}645$	0·996	±0·19
90	$L_{90} = 1{\cdot}999\, L_{eq} - 4{\cdot}568$	0·995	±0·21
95	$L_{95} = 0{\cdot}982\, L_{eq} - 4{\cdot}336$	0·993	±0·24

G1 case and equation (1) gives acceptable predictions of the noise level cumulative distributions in the present L_{eq} range. The lower kurtosis in the G2 case is probably due to the more continuous and steadily fluctuating noise sources (Figure 6). The performance of the Pearson Type III and Weibull distributions is again not very satisfactory (Figure 13).

It is observed from Figure 14 that though the level distribution mode relative to the L_{eq} decreases with L_{eq} as in Figure 11, the variation is more significant than that in the G1 case. It is also noticed that the modes of the G2 noise level fluctuations are further below the corresponding L_{eq}'s as compared to those of the G1 fluctuations on average. As mentioned before and shown in Figure 6, the larger noise climates of the G2 data are due to the more dominating and frequent noise events, which raises the L_{eq} and L_{10} significantly, so that the site background noise becomes less important in the overall noise exposure. The mode of the noise level distribution is close to the low sound pressure level end and thus will be further away from the L_{eq} as the noise climate increases.

4.3. G3 NOISE LEVEL FLUCTUATIONS

This type of noise level fluctuations are commonly found at sites where the noise sources are interrupted but the site background noise levels are not too low when compared to those caused by the noise sources. Data shown in Table 5 and Figure 15 suggest again the existence of relatively linear relationships between percentile levels and L_{eq}, though the uncertainty ranges are increased and more data scattering is observed in Figure 15 compared to the results shown in Figures 9 and 12. Data scattering becomes more serious at low percentile levels (large N). These levels are related to the background noise of the sites and thus relatively large site-wise variations are expected. Equation (1) gives similar

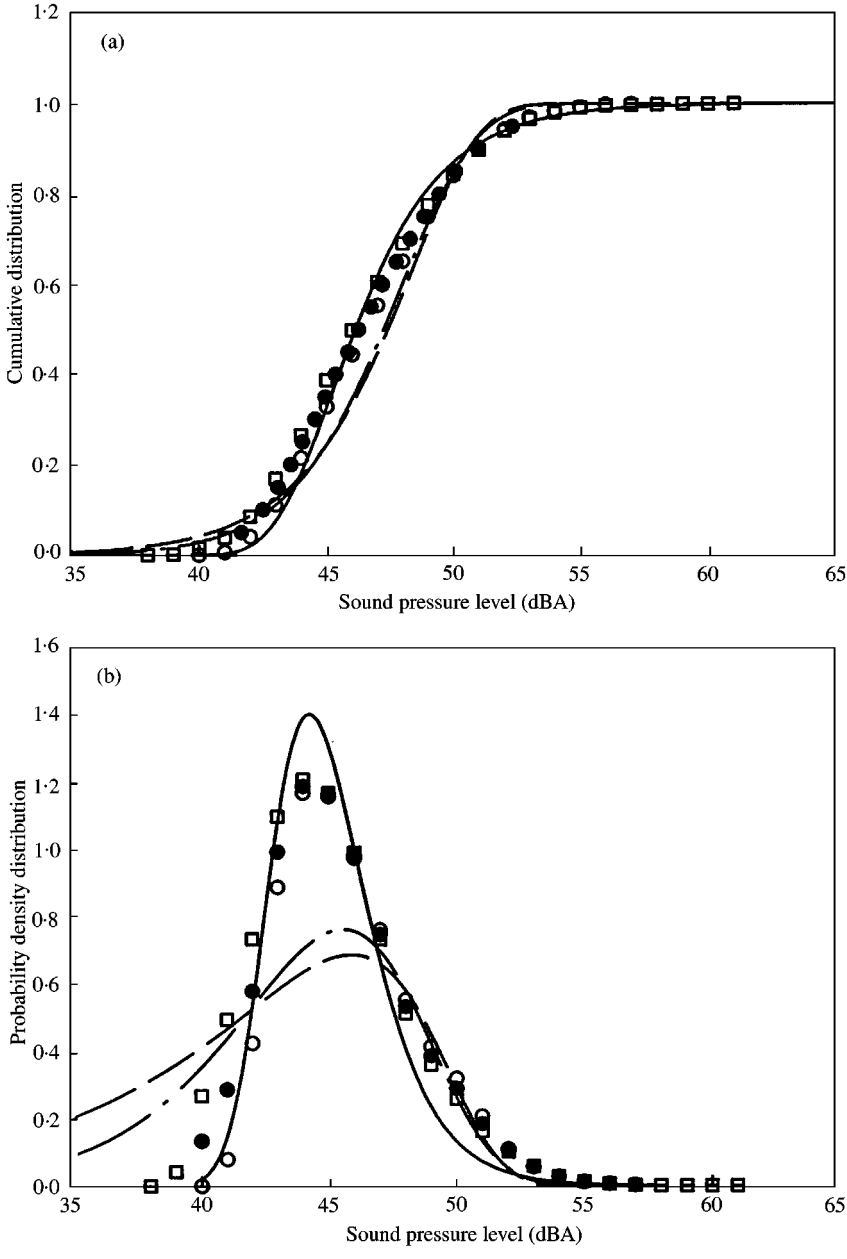

Figure 13. Example of a comparison between present model predictions and site measurements for G2 data. $L_{eq} = 47{\cdot}9$ dBA. (a) Noise level cumulative distribution; (b) noise level probability density distribution: ——, presented model; ○, □, measured results; ●, average of measured results; —·—, Pearson Type III distribution; — — —, Weibull distribution.

matching with the measured noise level cumulative distributions as in the G1 and G2 cases, though larger scattering is expected at the low noise level sides of the distributions. Thus, they are not presented. A 5 dB discrepancy between the modes of the measured noise level probability density distributions can be observed even with the same L_{eq} as shown in Figure 16. This is again expected as the mode at each site is close to the corresponding

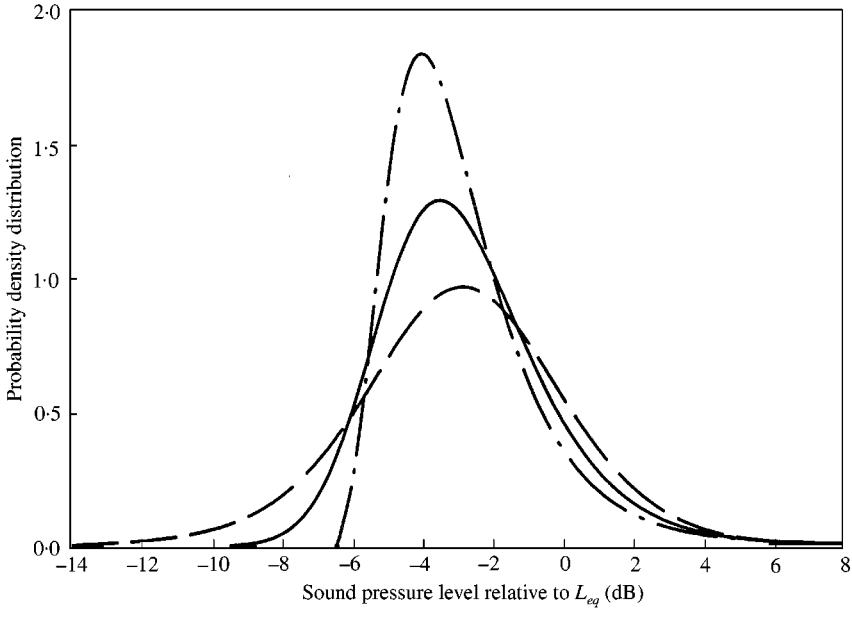

Figure 14. General trend of G2 data probability density distribution: —·—, $L_{eq} = 35$ dBA; ——, $L_{eq} = 52{\cdot}5$ dBA; — — —, $L_{eq} = 70$ dBA.

TABLE 5

Summary of linear relationships between L_N and L_{eq} for G3 data

N	Regression formula	Correlation coefficient R^2	Uncertainty range e (dB)
5	$L_5 = 0{\cdot}977\,L_{eq} + 7{\cdot}102$	0·989	±0·24
10	$L_{10} = 1{\cdot}032\,L_{eq} + 1{\cdot}537$	0·993	±0·20
15	$L_{15} = 1{\cdot}072\,L_{eq} - 2{\cdot}498$	0·989	±0·26
20	$L_{20} = 1{\cdot}100\,L_{eq} - 5{\cdot}356$	0·984	±0·32
25	$L_{25} = 1{\cdot}114\,L_{eq} - 7{\cdot}078$	0·983	±0·34
30	$L_{30} = 1{\cdot}121\,L_{eq} - 8{\cdot}260$	0·982	±0·35
35	$L_{35} = 1{\cdot}127\,L_{eq} - 9{\cdot}260$	0·981	±0·36
40	$L_{40} = 1{\cdot}126\,L_{eq} - 9{\cdot}874$	0·983	±0·35
45	$L_{45} = 1{\cdot}123\,L_{eq} - 10{\cdot}227$	0·983	±0·34
50	$L_{50} = 1{\cdot}120\,L_{eq} - 10{\cdot}573$	0·984	±0·33
55	$L_{55} = 1{\cdot}113\,L_{eq} - 10{\cdot}690$	0·985	±0·32
60	$L_{60} = 1{\cdot}104\,L_{eq} - 10{\cdot}646$	0·985	±0·32
65	$L_{65} = 1{\cdot}094\,L_{eq} - 10{\cdot}566$	0·984	±0·32
70	$L_{70} = 1{\cdot}085\,L_{eq} - 10{\cdot}546$	0·984	±0·32
75	$L_{75} = 1{\cdot}076\,L_{eq} - 10{\cdot}521$	0·984	±0·32
80	$L_{80} = 1{\cdot}066\,L_{eq} - 10{\cdot}494$	0·983	±0·33
85	$L_{85} = 1{\cdot}055\,L_{eq} - 10{\cdot}408$	0·982	±0·33
90	$L_{90} = 1{\cdot}045\,L_{eq} - 10{\cdot}467$	0·980	±0·34
95	$L_{95} = 1{\cdot}029\,L_{eq} - 10{\cdot}404$	0·978	±0·36

background noise level in this G3 data group. However, the present prediction still gives the mode and approximately the shape of the averaged result. The performance of the Pearson Type III and Weibull distributions is again not satisfactory and the corresponding results are not presented.

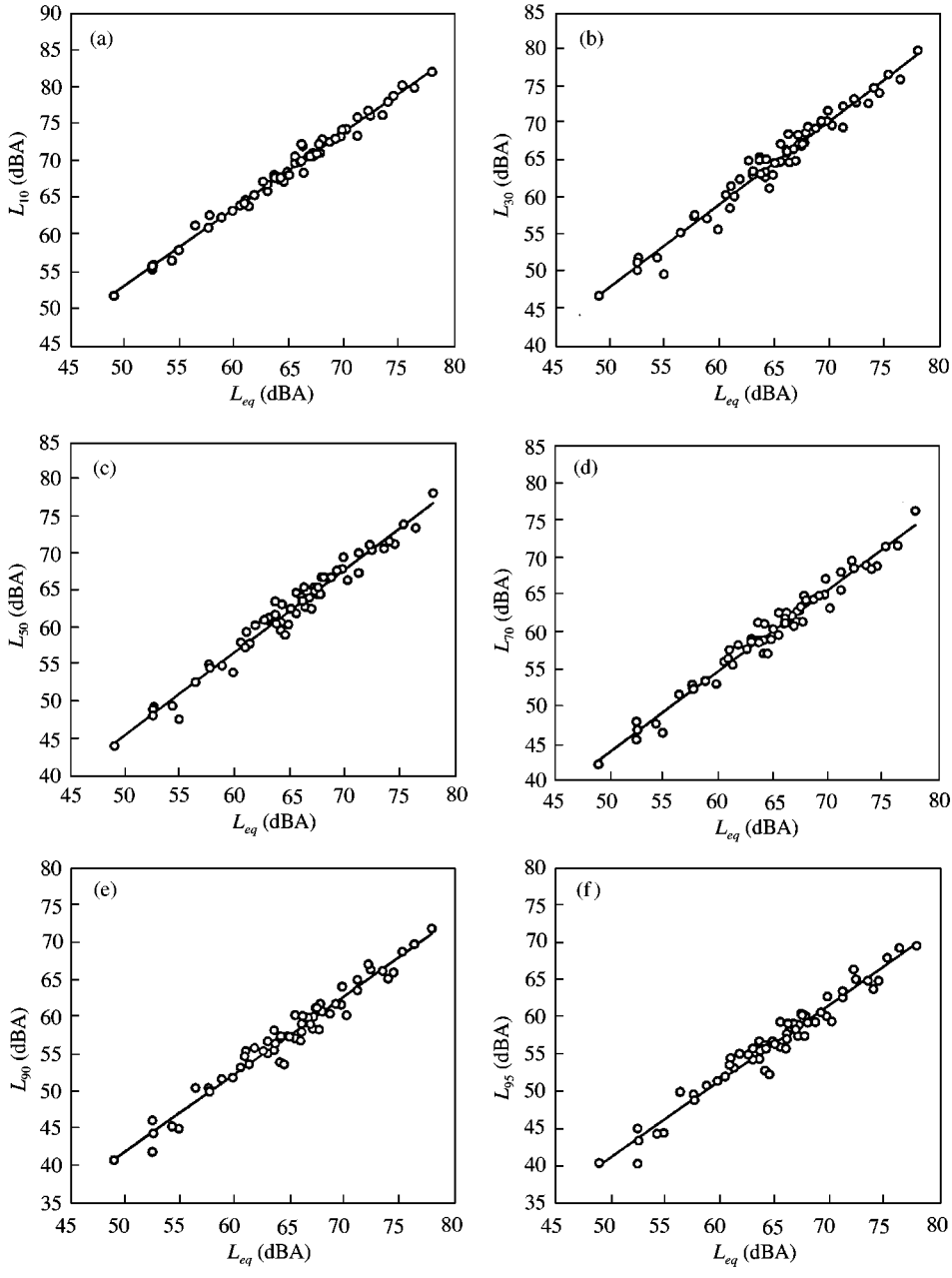

Figure 15. Linear relationships between percentile levels and L_{eq} and G3 data group. (a) L_{10}; (b) L_{30}; (c) L_{50}; (d) L_{70}; (e) L_{90}; (f) L_{95}: ——, regression lines; ○, measured data.

Figure 17 illustrates again the averaged G3 probability density distribution becomes more positively skewed as L_{eq} decreases as in the two previous data groups. At high L_{eq}, the distribution is more symmetrical about the mode, though not exactly of the Gaussian type. At very low L_{eq}, the distribution consists of a sharp rise to the mode followed by an immediate smoother fall and a long tail (not shown here). These are the characteristics of this G3 data group. At low L_{eq}, the large noise climate tends to imply relative long duration

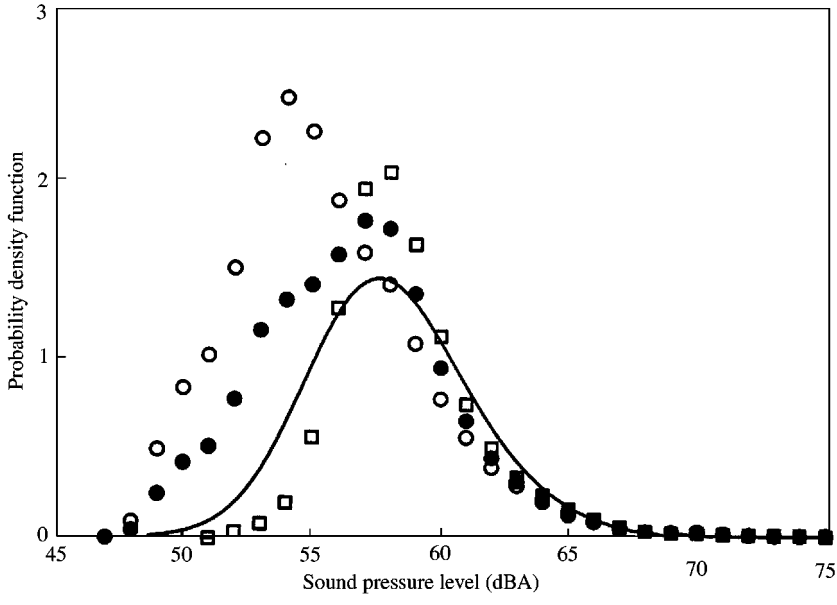

Figure 16. Example of a comparison between measured probability density distributions with prediction from equation (2). $L_{eq} = 64{\cdot}1$ dBA: ——, equation (2); ○, □, measured results; ●, average of measured results.

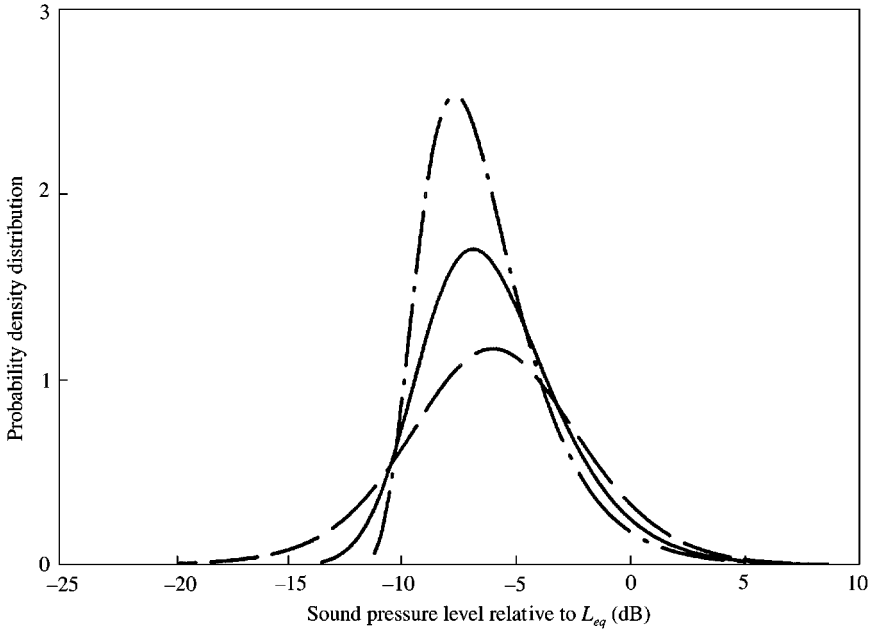

Figure 17. General trend of G3 data probability density distribution: —·—, $L_{eq} = 50$ dBA; ——, $L_{eq} = 60$ dBA; — — —, $L_{eq} = 70$ dBA.

of low noise level exposure with significant interrupted high noise energy events, such that there is a very high probability of having low noise levels in the measurements. The modes are further away from L_{eq} as expected and discussed in the previous section.

4.4. G4 NOISE LEVEL FLUCTUATIONS

Table 6 and Figure 18 suggest higher degree of data scattering and thus, larger mismatch between predictions and individual measured data sets, though the linear relationships between percentile levels and L_{eq} are still justified in the statistical sense. Some comparisons between predictions from equation (1) and the measured cumulative distributions are given in Figure 19(a). It can be observed that equation (1) does not always predict the shapes of the measured cumulative distributions. Although considerable differences between equation (2) predictions and the recorded noise level probability density distributions are observed (Figure 19(b)), the present model still gives the mode of the noise level probability density distribution within a 1 dB tolerance for most of the data recorded at sites. It is noticed that the predicted noise level probability density distribution has a significant portion at the low sound pressure level side for large L_{eq}, which is not observed in the recorded data and in the previous sections. The reason for this is unknown, but it may be due to accuracy of the recorded data, which are rounded up to the first decimal place by the sound level analyzer.

Figure 19(b) also suggests that the mode of the probability density distribution is about 10 dB below L_{eq}. The contribution of the quiet site background is very significant in this G4 cases. This is consistent with the previous discussions and Figure 8.

5. DATA FROM OTHER CITIES

Although the present study is carried out in the residential areas of Hong Kong, the existence of approximately linear relationships between the percentile levels and L_{eq} is not limited to the Hong Kong residential situation. Data from other cities are compared with the present data in this section. However, owing to the large volume of data available in the

TABLE 6

Summary of linear relationships between L_N and L_{eq} for G4 data

N	Regression formula	Correlation coefficient R^2	Uncertainty range e (dB)
5	$L_5 = 0{\cdot}976\, L_{eq} + 8{\cdot}058$	0·993	±0·50
10	$L_{10} = 0{\cdot}987\, L_{eq} + 5{\cdot}336$	0·994	±0·48
15	$L_{15} = 1{\cdot}006\, L_{eq} + 2{\cdot}574$	0·995	±0·44
20	$L_{20} = 1{\cdot}001\, L_{eq} + 1{\cdot}473$	0·995	±0·42
25	$L_{25} = 1{\cdot}006\, L_{eq} - 0{\cdot}044$	0·993	±0·52
30	$L_{30} = 1{\cdot}028\, L_{eq} - 2{\cdot}497$	0·992	±0·59
35	$L_{35} = 1{\cdot}041\, L_{eq} - 4{\cdot}302$	0·991	±0·63
40	$L_{40} = 1{\cdot}041\, L_{eq} - 5{\cdot}252$	0·989	±0·69
45	$L_{45} = 1{\cdot}039\, L_{eq} - 6{\cdot}004$	0·987	±0·75
50	$L_{50} = 1{\cdot}026\, L_{eq} - 6{\cdot}090$	0·985	±0·81
55	$L_{55} = 1{\cdot}017\, L_{eq} - 6{\cdot}408$	0·982	±0·87
60	$L_{60} = 1{\cdot}009\, L_{eq} - 6{\cdot}756$	0·980	±0·90
65	$L_{65} = 0{\cdot}992\, L_{eq} - 6{\cdot}532$	0·980	±0·90
70	$L_{70} = 0{\cdot}947\, L_{eq} - 6{\cdot}208$	0·979	±0·89
75	$L_{75} = 0{\cdot}965\, L_{eq} - 6{\cdot}509$	0·980	±0·86
80	$L_{80} = 0{\cdot}953\, L_{eq} - 6{\cdot}734$	0·982	±0·82
85	$L_{85} = 0{\cdot}949\, L_{eq} - 7{\cdot}493$	0·980	±0·85
90	$L_{90} = 0{\cdot}951\, L_{eq} - 8{\cdot}814$	0·977	±0·92
95	$L_{95} = 0{\cdot}940\, L_{eq} - 9{\cdot}518$	0·969	±1·05

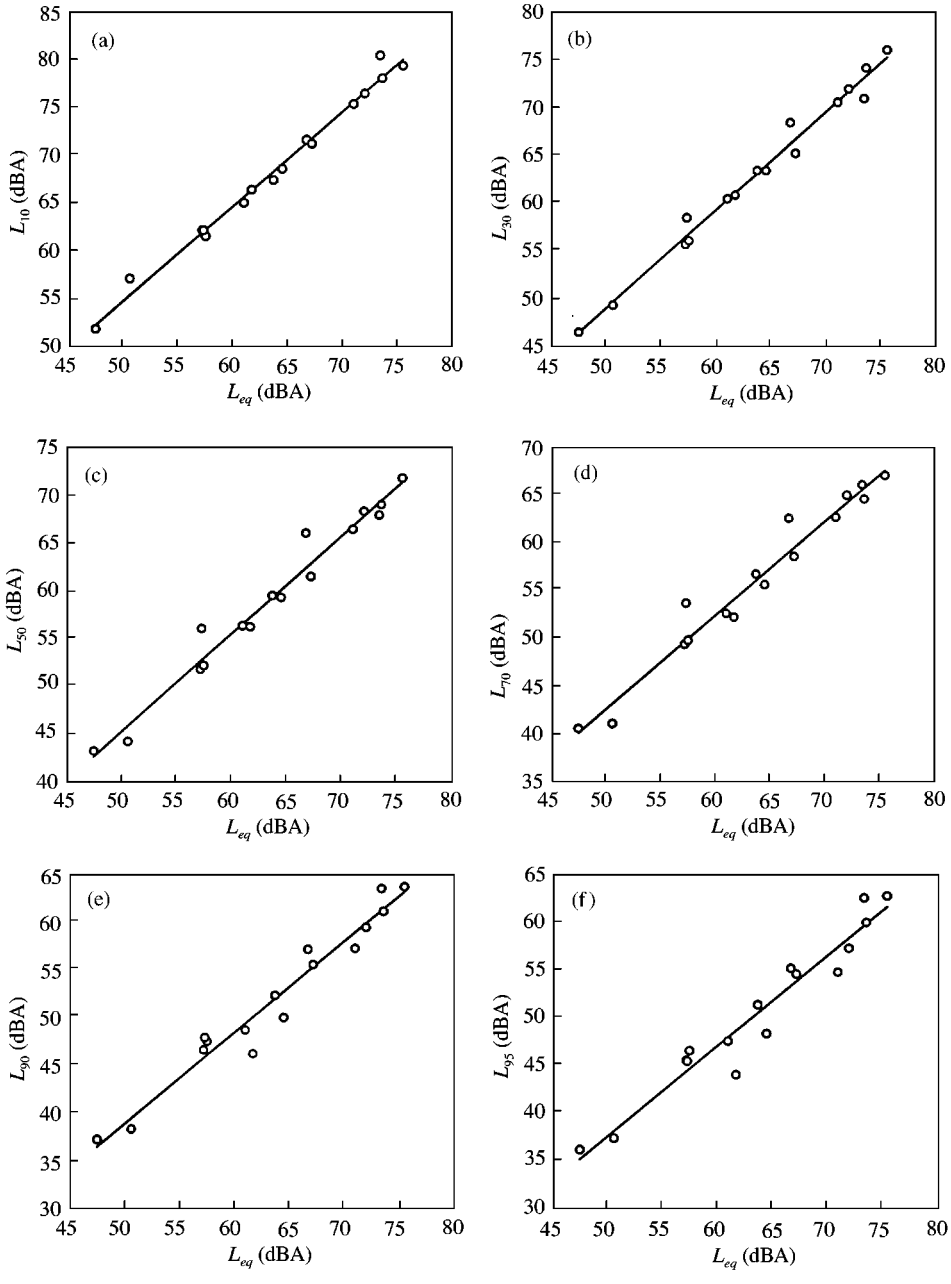

Figure 18. Linear relationships between percentile levels and L_{eq} and G4 data group. (a) L_{10}; (b) L_{30}; (c) L_{50}; (d) L_{70}; (e) L_{90}; (f) L_{95}: ——, regression lines; ○, measured data.

existing literature, the comparison here is by no means exhaustive. Also, only recent data will be considered.

The noise data of Chakrabarty *et al.* [1] recorded in 24 different locations in the city of Calcutta suggest the existence of similar linear relationships as far as L_{10} and L_{50} are concerned (Figure 20(a)), though it is not explicitly stated by the authors. Larger scattering

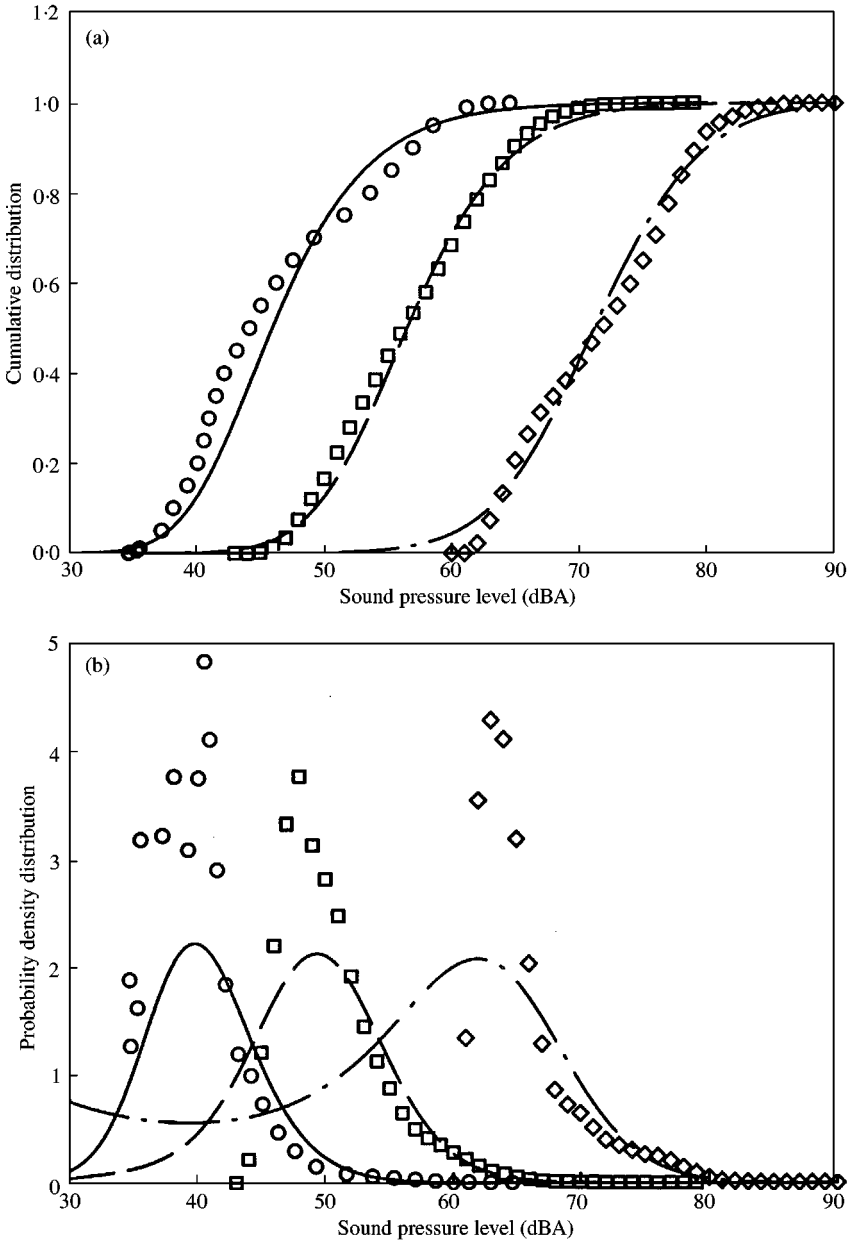

Figure 19. Comparisons between present model predictions and site measurements for G4 data. (a) Noise level cumulative distribution; (b) noise level probability density distribution: ——, —·—, — — —, present model predictions; ○, □, ◇, measured results.

is observed when L_{90} is considered. The L_{eq} data in the study of Chakrabarty *et al.* [1] are considerably higher than those in the present study, but its range is narrow ($\sim$10 dB) and the minimum noise climate is 18·8 dB, which is even higher than the maximum G4 data noise climate in the present study (19 dB). However, the matching between the present G4 L_{10} data and those of Chakrabarty *et al.* [1] is acceptable (Figure 20(a)). The slight change in the slope of the L_{50} line may be due to the very large noise climate in Calcutta so that the

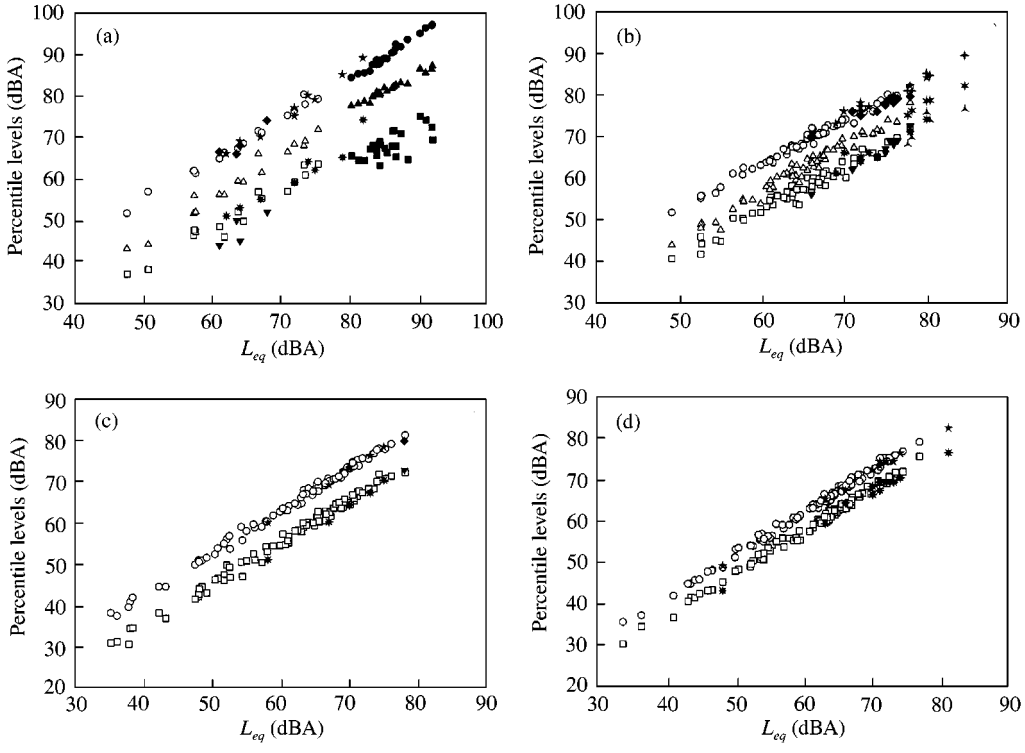

Figure 20. Comparisons between present data with those from other cites. (a) G4 data group; (b) G3 data group; (b) G2 data group; (b) G1 data group. Present data: ○, L_{10}; △, L_{50}; □, L_{90}. Chakrabarty *et al.* (Calcutta) [1]: ●, L_{10}; ▲, L_{50}; ■, L_{90}. Onuu (south-east Nigeria) [4]: ∗, L_{10}; ★, L_{50}; ∗, L_{90}. Arana and Garcia (Pamplona) [17]: ◆, L_{10}; ▼, L_{90}. Saadu *et al.* (Nigeria) [18]: ★, L_{10}; ∗, L_{90}.

data may not actually belong to the G4 group. However, the regression line that fits both the present data and those of Chakrabarty *et al.* [1] has a correlation coefficient of 0·992 and the uncertainty range is $\pm$ 0·36 dB. This suggests that a linear relationship between L_{50} and L_{eq} is still justified even when the Calcutta data are included.

The noise data obtained in several south-east Nigerian cities also suggest the existence of a linear relationship between percentile levels and L_{eq} [4]. Excluding the data of Onuu [4] having $(L_{eq} - L_{50})/(L_{10} - L_{50}) > 0{\cdot}75$, which are believed to be abnormal and not representative, most of the presented Nigerian data have noise climates between 9 and 14 dB (G3 in the present classification). Figure 20(b) illustrates a comparison between these Nigerian data and the present G3 data. The former appears to be an extension of the present G3 data to a higher L_{eq} region.

The results of hourly L_{eq}, L_{10} and L_{90} measurements carried out by Arana and Gracía [17] in the busy residential areas of the city Pamplona contain mainly G3 and G4 type data, where one set belongs to the G2 type. Their agreement with the present data is good (Figure 20(a)–20(c)). Four Pamplona data are rejected as the corresponding L_{eq} is very close to L_{10}. The quiet Pamplona data are not included in the comparison here because most of the L_{eq} in this data set is close to or even exceeds L_{10}. The results of Saadu *et al.* [18] contains all the four types of noise level fluctuations found in the present study. Again, those data with L_{eq} close to L_{10} are ignored. It can be observed from Figure 20(a)–20(d) that their matching with the present data is very acceptable.

The results of Burgess [15] also suggest the existence of a linear relationship between L_{10} and L_{eq}. However, these results were obtained in the late 1970s and thus are not discussed here. Gracía and Garrigues [19] have presented another set of noise data obtained in Spain. However, most of the L_{eq} in their results are close to L_{10}, making the ratio of $(L_{eq} - L_{50})/(L_{10} - L_{50})$ very close to or exceeding 0·75. A comparison with the present results thus appears difficult. The arithmetic mean noise data as presented in Gracía and Garrigues [19] may not provide the true relationships between percentile levels and L_{eq}, which must be studied through direct one-to-one mapping of L_{eq} to the corresponding set of percentile levels. Indeed, the results of Gracía and Garrigues [19] also reveal the possibility of linear relationships between the percentile levels and L_{eq}. However, their data match more to the present G4 data though the corresponding noise climates are less than 14 dB. This may be due to the arithmetic averaging of noise levels taken by Gracía and Garrigues [19].

The comparisons made in this section suggest that the environmental noise is not as random as one is expecting. Similar linear relationships between the percentile levels and L_{eq} are also found in other cities. The results confirm the suitability of using noise climate for outdoor noise data classification. The distribution function proposed by Tang [10] appears applicable not just in Hong Kong, especially for the prediction of L_{10}.

6. CONCLUSIONS

In the present study, outdoor noise levels were recorded in Hong Kong at 275 residential locations having a large variety of noise sources and the degree to which these sources were affecting the local environments. The noise level time variation patterns were also examined. In addition, the relationships between the percentile levels and the equivalent sound pressure levels are studied. Besides, the application of the noise level distribution function proposed previously by the author in outdoor situations is discussed.

The relationships between the percentile levels and the equivalent sound pressure levels suggest that the use of residential area types and the degree of noise sources affecting the outdoor environments is not able to describe the characteristics of the noise level time fluctuations obtained. The results illustrate that the noise climate is a better parameter and its probability distribution shows that there exist four groups of noise level fluctuations in the present study, within which linear relationships between percentile levels and the equivalent sound pressure levels are justified by statistical means. The distribution function proposed previously by the author, though with no concrete theoretical proof, gives reasonable predictions for the noise climate less than 9 dB. Although the degree of mismatch between predictions and measurements in general increases with noise climate afterward, the proposed function predicts the modes of most of the noise level probability density functions in all the four data groups within engineering tolerance. It is also found that the proposed distribution function does not work in the cases where the noise environment is dominated by limited strong noise events which cause equivalent sound pressure level close to or even larger than the L_{10}. However, these circumstances are all not representative in normal residential areas in Hong Kong.

To conclude, it has been shown that the previously proposed distribution function by the author, which is originally developed for use in the indoor built environment, can be applied also in the outdoor residential environment. This suggests further its generality. Although the present study was done in Hong Kong, it is believed that the function is also applicable in other cities since similar relationships between percentile levels and equivalent sound pressure levels have been observed at least in Calcutta of India, Pamplona of Spain and several Nigerian cities.

ACKNOWLEDGMENTS

SKT would like to thank the Research Committee, the Hong Kong Polytechnic University for the financial support during the course of the work.

REFERENCES

1. D. CHAKRABARTY, S. C. SANTRA, A. MUKHERJEE, B. ROY and P. DAS 1997 *Journal of the Acoustical Society of America* **101**, 943–949. Status of road traffic noise in Calcutta metropolis, India.
2. G. J. WADSWORTH and J. P. CHAMBERS 2000 *Journal of the Acoustical Society of America* **107**, 2344–2350. Scale model experiments on the insertion loss of wide and double barriers.
3. U. J. KURZE 1971 *Journal of Sound and Vibration* **18**, 171–195. Statistics of road traffic noise.
4. M. U. ONUU 2000 *Journal of Sound and Vibration* **233**, 391–405. Road traffic noise in Nigeria: measurements, analysis and evaluation of nuisance.
5. J. FOXON and F. J. PEARSON 1968 *Applied Acoustics* **1**, 175–188. A statistical model of traffic noise.
6. C. G. DON and I. G. REES 1985 *Journal of Sound and Vibration* **100**, 41–53. Road traffic sound level distributions.
7. W. E. SCHOLES 1970 *Applied Acoustics* **3**, 1–21. Traffic noise criteria.
8. D. W. ROBINSON 1971 *Journal of Sound and Vibration* **14**, 279–298. Towards a unified system of noise assessment.
9. S. K. TANG and W. H. AU 1999 *Journal of the Acoustical Society of America* **106**, 3415–3423. Statistical structures of indoor traffic noise in a high rise city.
10. S. K. TANG 1997 *Journal of Sound and Vibration* **208**, 603–615. A distribution function applicable to office noise study.
11. S. K. TANG and Y. S. CHOY 1998 *Journal of Sound and Vibration* **218**, 599–604. Further investigation on noise distribution function.
12. W. P. ELDERTON and N. L. JOHNSON 1969 *Systems of Frequency Curves*. Cambridge: Cambridge University Press.
13. W. WEIBULL 1951 *Transactions of the American Society of Mechanical Engineers*: *Journal of Applied Mechanics* **18**, 293–297. A statistical distribution function of wide applicability.
14. F. J. FAHY 1994 *Philosophical Transactions of the Royal Society of London*, *Series A* **346**, 431–447. Statistical energy analysis: a critical overview.
15. M. BURGESS 1978 *Australian Road Research* **8**, 15–18. Relationship between L_{10} and L_{eq} for noise from road traffic.
16. R. J. JESSEN 1978 *Statistical Survey Techniques*. New York: Wiley.
17. M. ARANA and A. GARCÍA 1998 *Applied Acoustics* **53**, 245–253. A social survey on the effects of environmental noise on the residents of Pamplona, Spain.
18. A. A. SAADU, R. O. ONYEONWU, E. O. AYORINDE and F. O. OGISI 1998 *Noise Control Engineering Journal* **46**, 146–158. Road traffic noise survey and analysis of some major urban centers in Nigeria.
19. A. GARCÍA and J. V. GARRIGUES 1998 *Noise Control Engineering Journal* **46**, 159–166. 24-hour continuous sound-level measurements conducted in Spanish urban areas.